



Satellite-Based Time Series of Chlorophyll in Chilko Lake, British Columbia, Canada

Leslie N. Brown, Gary A. Borstad, Kaan Ersahin, Eduardo Loos, Daniel Selbie, Maycira Costa & James R. Irvine

To cite this article: Leslie N. Brown, Gary A. Borstad, Kaan Ersahin, Eduardo Loos, Daniel Selbie, Maycira Costa & James R. Irvine (2019) Satellite-Based Time Series of Chlorophyll in Chilko Lake, British Columbia, Canada, Canadian Journal of Remote Sensing, 45:3-4, 368-385, DOI: [10.1080/07038992.2019.1632699](https://doi.org/10.1080/07038992.2019.1632699)

To link to this article: <https://doi.org/10.1080/07038992.2019.1632699>



© 2019 The Author(s). Published by Informa UK Limited, trading as Taylor & Francis Group



Published online: 15 Jul 2019.



Submit your article to this journal [↗](#)



Article views: 291



View related articles [↗](#)



View Crossmark data [↗](#)

Satellite-Based Time Series of Chlorophyll in Chilko Lake, British Columbia, Canada

Leslie N. Brown^a, Gary A. Borstad^a, Kaan Ersahin^a, Eduardo Loos^{a,b}, Daniel Selbie^c, Maycira Costa^d, and James R. Irvine^e

^aASL Environmental Sciences Inc, Victoria, British Columbia, Canada; ^bNow at Vertex Resource Group, Victoria, British Columbia, Canada; ^cFisheries and Oceans Canada, Salmon Research Laboratory, Cultus Lake, British Columbia, Canada; ^dUniversity of Victoria, Victoria, British Columbia, Canada; ^eFisheries and Oceans Canada, Nanaimo, British Columbia, Canada

ABSTRACT

In Canada, many northern lakes are remote and difficult to access, with limited limnological data. Satellite sensors provide widespread coverage and growing time series of data unavailable via conventional sampling, but global validation is still limited. We evaluated chlorophyll estimates from the MERIS (Medium Resolution Imaging Spectrometer) sensor on board the European Space Agency (ESA) ENVISAT satellite for the ultra-oligotrophic Chilko Lake in the coastal mountains of central British Columbia. This lake supports a valuable sockeye salmon (*Oncorhynchus nerka*) population. We obtained good temporal coverage, through 1,425 scenes between June 18, 2002 and April 6, 2012. Although pre-processing was required to produce a high-quality dataset, one standard ESA algorithm generated chlorophyll estimates similar to field data. Regional and interannual phenological patterns were clear, and differences that may be important determinants of salmon production were well described. Although MERIS ceased operation in April 2012, it was replaced by the OLCI (Ocean and Land Color Instrument) on the SENTINEL 3a and 3b satellites launched in February 2016 and April 2018, respectively. We conclude that, with appropriate quality control and *in situ* validation, satellite-generated chlorophyll time series in sockeye salmon rearing lakes have significant potential as a fisheries planning and analysis tool.

RÉSUMÉ

Au Canada, de nombreux lacs nordiques sont éloignées et difficiles d'accès, avec des données limnologiques limitées. Les capteurs satellites fournissent une couverture étendue et une série chronologique croissante de données non disponibles via l'échantillonnage conventionnel, mais la validation globale est encore limitée. Nous avons évalué les estimations de la chlorophylle à l'aide du capteur MERIS (spectromètre imageur à résolution moyenne) à bord du satellite ENVISAT de l'Agence Spatiale Européenne pour le lac Chilko, un lac ultra-oligotrophe dans les montagnes côtières du centre de la Colombie-Britannique. Ce lac abrite une population de saumon rouge (*Oncorhynchus nerka*). Nous avons obtenu une bonne couverture temporelle, soit 1425 scènes entre le 18 juin 2002 et le 6 avril 2012. Bien qu'un prétraitement ait été nécessaire pour produire un jeu de données de haute qualité, un algorithme standard de l'ESA a généré des estimations de la chlorophylle similaires aux données de terrain. Les schémas phénologiques régionaux et interannuels étaient clairs et les pouvant être des déterminants importants pour la production de saumon étaient bien décrites. Bien que MERIS ait cessé ses activités en avril 2012, il a été remplacé par les instruments OLCI (Ocean and Land Color Instrument) des satellites SENTINEL 3a et 3b lancés respectivement en février 2016 et en avril 2018. En conclusion, avec un contrôle de qualité approprié et une validation *in situ*, les séries chronologiques de chlorophylle générées par satellite dans les lacs d'élevage de saumon rouge présentent un potentiel important en tant qu'outil de planification et d'analyse des pêches.

ARTICLE HISTORY

Received 15 January 2019
Accepted 13 June 2019

Introduction

Chilko Lake, within the Fraser River watershed, hosts one of the most valuable sockeye salmon

(*Oncorhynchus nerka*) populations in British Columbia (BC), contributing significantly to commercial, recreational and indigenous fisheries. Chilko

CONTACT Kaan Ersahin  kersahin@aslenv.com

© 2019 The Author(s). Published by Informa UK Limited, trading as Taylor & Francis Group
This is an Open Access article distributed under the terms of the Creative Commons Attribution-NonCommercial-NoDerivatives License (<http://creativecommons.org/licenses/by-nc-nd/4.0/>), which permits non-commercial re-use, distribution, and reproduction in any medium, provided the original work is properly cited, and is not altered, transformed, or built upon in any way.

sockeye salmon typically exhibit a 4-year life cycle, spending their first 2 years in freshwater (i.e., incubation and rearing environments) feeding primarily on zooplankton before migrating to the ocean to mature, returning approximately 2 years later to spawn and die (Akenhead et al. 2016). Similar to most northern lakes, long-term limnological data for Chilko Lake are temporally limited and discontinuous relative to commensurate fisheries data. As such, this study set out to test whether satellite Earth Observation (EO) generated data were of sufficient quality and quantity to supplement existing *in situ* lake data, to provide quasi-continuous, archival records of lake chlorophyll useful for better understanding variability and change in the Chilko Lake ecosystem, and potential factors responsible for determining salmon survival.

There are challenges with the application of EO water color data for Chilko Lake. First, although it is one of the largest lakes in BC, it is long and narrow (5 km wide at its widest point), and surrounded by high-glaciated mountains. As a result, only satellite sensors with moderately high resolution are capable of providing useful information about spatial variability within the lake. Second, glacial turbidity, shading and adjacency effects from atmospheric scattering above the bright glaciers affect the data. The first and only remote-sensing study of the lake by Gallie and Murtha (1992) used Landsat because the Coastal Zone Color Scanner (CZCS), which was designed to image water and operated from 1978 to 1983, had only 1 km spatial resolution, making it unsuitable for imaging the narrow fjord-like Chilko Lake. Using Landsat, Gallie and Murtha (1992) were able to image the lake, and produced Inherent Optical Properties (IOPs) for suspended materials via chromaticity analysis. They were not able to derive chlorophyll and dissolved “yellow substance” (typically dissolved tannins and lignins from decomposition of terrestrial vegetation, that absorb most strongly absorbs short wavelength light, turning waters yellow-brown when present in high concentrations) because Landsat MSS did not then have appropriate spectral bands. Other sensors (SeaWiFS, MODIS, MERIS, and many others) with spectral bands designed to measure water color have been launched since. However, at the time this project was undertaken (2012–2013), MERIS Full Resolution (FR) was the only water color sensor with both appropriate spectral bands and sufficient spatial resolution (300 m).

Chilko Lake is large (surface area 185 km²), with a cool (mean temperature 8.2 C), deep epilimnion (mean depth 24.2 m) and depths of 100 to 300 m. The

lake has low nutrient loading and low spring overturn nitrate and phosphorous concentrations. As a result the lake is ultra-oligotrophic with exceptionally clear water and a deep euphotic zone. It is subjected to pulses of glacial turbidity in the southern half of the lake during the spring and early summer months (Shortreed et al. 2001; Stockner and Shortreed 1994; Hume et al. 1996). This means that *Case 1* algorithms (those intended for waters dominated by chlorophyll, with very low dissolved organic or suspended inorganic matter) may not accurately retrieve chlorophyll concentrations. A number of algorithms, have been developed to handle such conditions of high turbidity and/or high-dissolved organic load, including several designed specifically for use with MERIS data. These algorithms, collectively referred to as *Case 2 algorithms*, include neural network modeling approaches trained over a wide range of different water types such as the *Case 2 Regional* (C2R; Doerffer and Schiller 2007), *FUB/WeW* (Schroeder et al. 2007), and *Eutrophic and Boreal Lakes* (Doerffer and Schiller 2008) processors implemented as plug-in processors in BEAM. Validation studies in several lakes have demonstrated that the performance of individual algorithms varies widely among systems (e.g., Odermatt et al. 2010; Odermatt et al. 2012; Palmer et al. 2014; Palmer et al. 2015; Salem et al. 2017). Before using MERIS time series to describe lake dynamics, and in comparative analyses with fisheries data, there was a need to determine which, if any of these algorithms adequately capture chlorophyll concentrations in Chilko Lake. The goal of this study was to evaluate several Case 2 algorithms applied to MERIS imagery for the estimation of surface chlorophyll concentrations within the system. *In situ* measurements (i.e., extracted chlorophyll, spectroradiometry, fluorometry) acquired in 2009 to 2011 were used to validate the MERIS algorithms, supplement the satellite observations and infer primary production dynamics.

Methods

Study area

Chilko Lake is a large (70 km long, 3–5 km wide, surface area of 200 km²), ultra-oligotrophic, glacially fed lake, located on the eastern side of the Coast Mountain range in British Columbia (51° 15' N, 124° 05' W) at 1,172 m elevation (Figure 1). It is one of the largest lakes in the province in terms of volume due to its depth (mean 123 m, maximum 330 m), and the largest one above 1,000 m elevation. The lake waters develop seasonal turbidity along a south-to-north

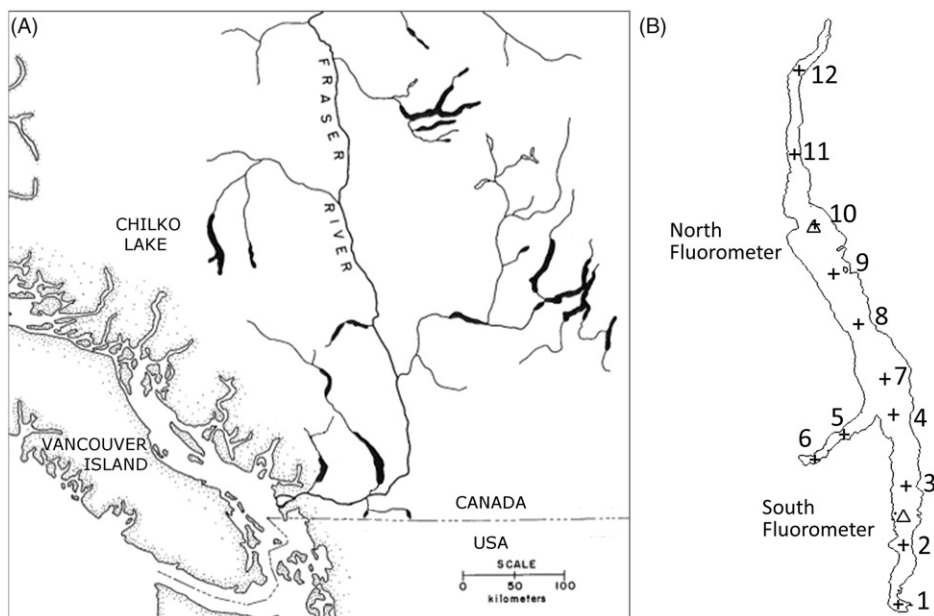


Figure 1. A. Location of Chilkco Lake and other salmon producing lakes in south central British Columbia, from Nidle et al. 1990. B. Chilkco Lake, showing and locations of sampling stations 1 to 12 and moored fluorometers (triangles). Note that the lake drains to the north and this outlet is an important spawning location.

gradient due to the discharge by glacially influenced rivers entering the southern half of the lake. Along with the high elevation of the system at the edge of the coastal mountains and the frequent, strong katabatic winds, these cold water inputs contribute to the typically low water surface temperatures (maximum summer temperatures of 14 °C). Winds play an important role in water circulation and associated turbidity patterns within the lake, and strongly influencing seasonal development of the thermal structure of the lake. During winter, the water column is vertically mixed, with spatiotemporally discontinuous inter-annual ice cover and does not typically stratify until July. Owing to strong forcing on the lake surface due to the high-alpine winds, summer thermal structure in the summer is dynamic, with epilimnion depths ranging between 10 m and 50 m as a result of internal searching and associated mixing, deflections, and oscillations of the thermocline (Hume et al. 1996).

Field data

In situ chlorophyll data used for the validation of satellite chlorophyll algorithms were obtained from historical limnological studies conducted by the Lakes Research Program (LRP) of Fisheries and Oceans Canada. Data from surface grab samples or near surface van Dorn samplers (0–0.5 m) were available for nine stations distributed along the main axis of the lake (Figure 1a). Chlorophyll *a* concentration was measured fluorometrically on 0.45 µm Millipore HA

membrane filters (folded in half and frozen for storage). At the time of analysis, the sample filters were macerated in 90% acetone and the supernatant analyzed fluorometrically according to the methods of Strickland and Parsons (1972) using a model 10-AU Turner Designs fluorometer. Turbidity was measured by nephelometry on 1 L samples (American Public Health Association 1998) on a la Motte 2020 turbidity meter. Colored Dissolved Organic Material (CDOM), measured spectrophotometrically was only available from the sampling visit during 2012. Ninety-five match-ups were obtained between *in situ* data and 16 MERIS image scenes between July 16, 2009 and October 6, 2011.

In addition to the DFO-LRP monthly sampling, two Wetlabs ECO-FLNTUSB fluorometers were moored at either end of the lake to provide continuous estimates of chlorophyll and turbidity between May 19 and October 11, 2012 (Figure 1b). This instrument measures chlorophyll fluorescence at 695 nm (excitation at 470 nm) and turbidity from optical backscatter at 700 nm. The northern mooring was at a depth of 5.3 m \pm 0.3 (1 SD), but bad weather at the time of the mooring meant that the southern mooring was finally situated at 2.98 m \pm 0.3 (1 SD). The depth differences are not significant given that the euphotic depth averages 25–29 m. Also, these data were acquired after the unexpected end of the MERIS mission and so were not used for validation. They were, however useful for evaluating the time scales of variability of these two parameters in Chilkco Lake.

Table 1. Concentration calibration ranges for the C2R, boreal lakes and FUB/WeW algorithms. Also shown for reference are the ranges of values measured in Chilko Lake surface waters between 2009 and 2011 (CDOM was not measured), and reported in the literature.

| Algorithm | chl-a (mg .m ⁻³) | TSM ^a (g .m ⁻³) | CDOM (a440 m ⁻¹) | Reference |
|------------------------------------|---------------------------------|---|---------------------------------|-------------------------------|
| C2R | 0.016–43.2 | 0.0087–51.9 | 0.005–5.0 | Doerffer and Schiller (2007) |
| C2RB | 0.5–50 | 0.1–20 | 0.25–10 | Koponen et al. (2008) |
| FUB/WeW | 0.05–50 | 0.05–50 | 0.005–1.0 | Schroeder and Fischer (2003) |
| Chilko <i>in situ</i> ^b | | | | |
| 2009–2011 | 0.02–1.17 | 0.00–6.41 | | This study |
| 1984–1986 | 0.19–0.36 | 0.66–23.39 | 0.10–0.82 | Gallie and Murtha (1992) |
| May-Oct 1985 | 0.24–1.54 | | | Stockner and Shortreed (1994) |
| May-Oct 1986 | 0.23–0.79 ^c | | | Nidle et al. (1990) |

^aChilko TSM values were converted from turbidity in NTU based on an intercalibration performed from 2012 field data.

^bChilko Lake was the site of whole lake fertilization experiments during the 1990s. Only data from unfertilized years is shown here.

^cChlorophyll reported by Nidle and Stockner is mean epilimnetic chlorophyll.

MERIS-based chlorophyll algorithms: Description, processing and validation

Algorithm descriptions

Three Case 2 water color algorithms were assessed for applicability in Chilko Lake: the Case 2 Regional (C2R) processor (Doerffer and Schiller 2007), including its Boreal lakes variant (C2RB), and the FUB/WeW processor from the Free University of Berlin (Schroeder et al. 2007). C2R and C2RB were trained using sequential neural networks to first perform atmospheric correction and then retrieve Inherent Optical Properties (IOPs) from which concentrations of chlorophyll, Suspended Particulate Matter (SPM), and absorption due to Colored Dissolved Organic Matter (CDOM) are derived. The neural networks used to perform the atmospheric correction for both algorithms were trained using radiative transfer modeling based on HYDROLIGHT (Mobley 1994). The two algorithms differ in the bio-optical properties used to characterize the three components (chlorophyll, SPM and CDOM): for C2R these are based on observations from the North Sea, Baltic Sea, Mediterranean Sea and North Atlantic (Doerffer and Schiller 2007), and for the C2RB algorithm, observations from Finnish lakes were used (Koponen et al. 2008). Two versions of the algorithms were tested, versions 1.3.2 and 1.4.1 for C2R, and versions 1.0.2 and 1.4.1 for C2RB. Although v1.4.1 of both algorithms were the current versions at the time of data processing, preliminary testing suggested superior performance of the older versions, hence both older and newer versions were included in the analysis. Differences between the versions include inclusion of polarization effects and improvements to glint correction in version 1.4.1 (Brockmann Consult 2015).

The FUB/WeW processor also uses neural networks to both perform atmospheric correction and retrieval of the three optical constituents. The

atmospheric model is based on the radiative transfer code of Fischer and Grassl (1984) and Fell and Fischer (2001). Optical properties used for this model were derived chiefly from ultra-oligotrophic to mesotrophic Case 1 waters for chlorophyll (Schroeder et al. 2007; Bricaud et al. 1998), and European coastal waters for SPM and CDOM (Babin 2000). Table 1 summarizes the concentration ranges of the datasets reported by the authors to train their algorithms. All three algorithms are implemented in ESA's Basic ENVISAT and AATSR MERIS (BEAM) toolbox (Fomferra and Brockmann 2005), which was used here to process the level 1B data to the level 2 products. Note that BEAM was replaced by SNAP (Sentinel Application Platform) in 2016. FUB appears to have remained, but major improvements to C2R were introduced as part of the CoastColour Project (Brockmann and Doerffer 2016), and C2R has been replaced by C2RCC (Case 2 Regional CoastColour).

Image processing

All available MERIS FR scenes with at least partial coverage of Chilko Lake were downloaded from ESA's Earth Observation Link (EOLi) archive for 2002 to 2007, or the Canada Centre for Mapping and Earth Observation (CCMEO) for 2008 to 2012, as level 1B top-of-atmosphere radiances. This amounted to 1,425 scenes spanning the period June 18, 2002 to April 6, 2012. Before the algorithms could be evaluated on the EO data, several pre-processing steps were required.

Navigation correction. Mapping of the level 2 products was performed using the Mosaic processor in BEAM version 4.7.1 provided by ESA specifically for processing MERIS and other ESA Earth Observation (EO) data that uses the tie point tables included in the level 1 product metadata to achieve a first-order correction. We found that because MERIS swaths were extremely wide (1150 km) and the lake is narrow, the variation in across-track pixel size

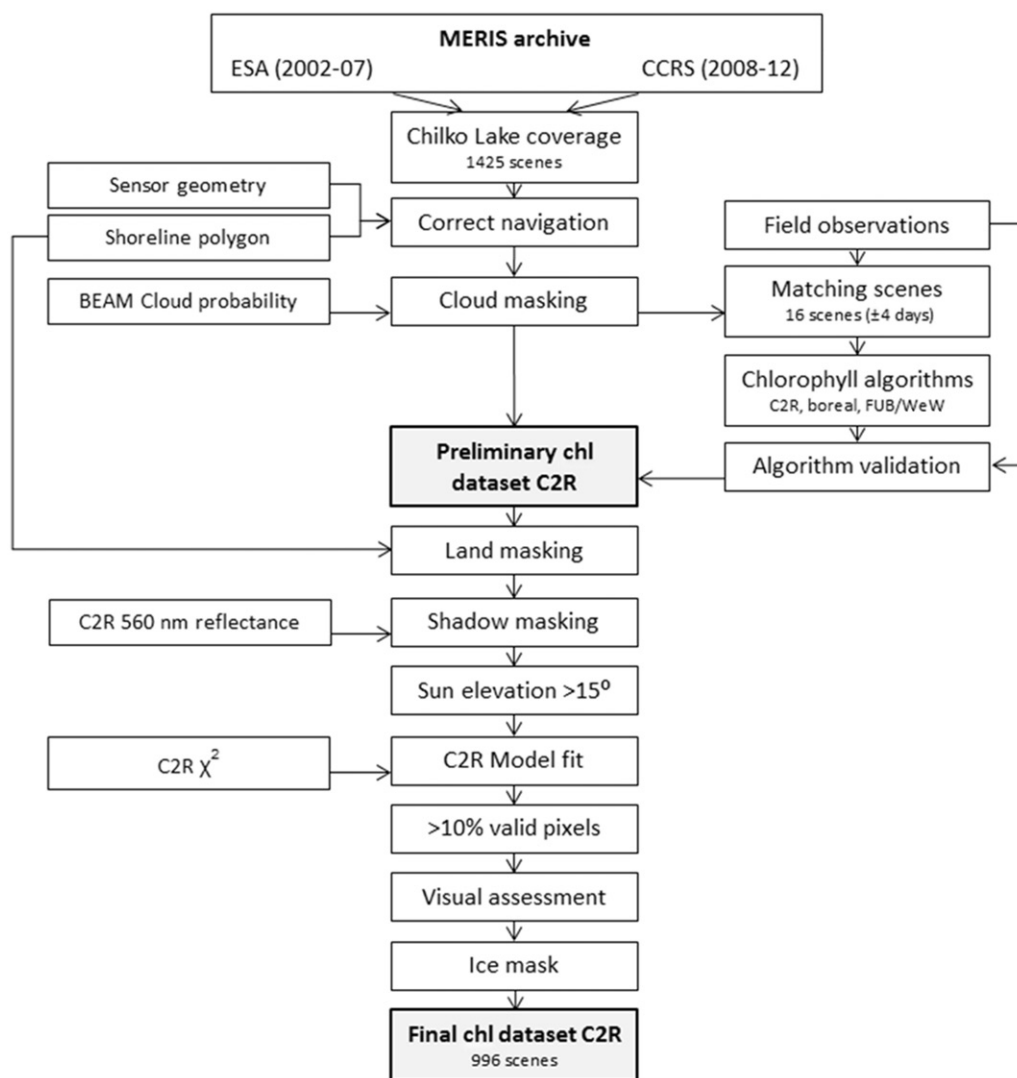


Figure 2. MERIS data processing including algorithm validation and compilation of a quality controlled time series.

associated with varying sensor geometry was significant, and an adjustment was required in order to precisely navigate each scene. An empirical adjustment was applied based on the fit of the imagery to a Chilko Lake provincial shoreline polygon (GeoBC 2008).

Cloud masking. Cloud masking was performed using the Cloud Probability Processor (CPP; Preusker et al. 2006), also implemented in BEAM 4.7.1, with all pixels having a cloud probability greater than 20% excluded from analysis. Although this is the most aggressive of the masking thresholds flagged by the CPP, it did not always capture all cloud-related errors. We experimented with further reductions in the threshold, but found that this resulted in an unacceptable loss of valid data, so the 20% threshold was retained. Imagery used for algorithm validation was visually inspected and any locations affected by unmasked cloud or other artifacts were excluded from

analysis. Further quality control flags were applied to the satellite image time series as explained below.

Algorithm retrieval validation

For algorithm validation, MERIS image matches acquired within a maximum of 4 days of each *in situ* measurement were selected, for a total of 16 scenes and 98 validation points. Ninety-four percent of image matchups were within 2 days of field sampling, and 68% were within one day. Medians of 3×3 pixel areas (approximately $750 \text{ m} \times 750 \text{ m}$) were extracted from the mapped image products for each station location for comparison with the field measurements. The 3×3 sample size was selected to allow for small navigation errors as well as water spatial dynamics during the intervals between image acquisition and field sampling, while avoiding the margins of this narrow lake. Median values rather than means were used in order to minimize the effects of small localized features such

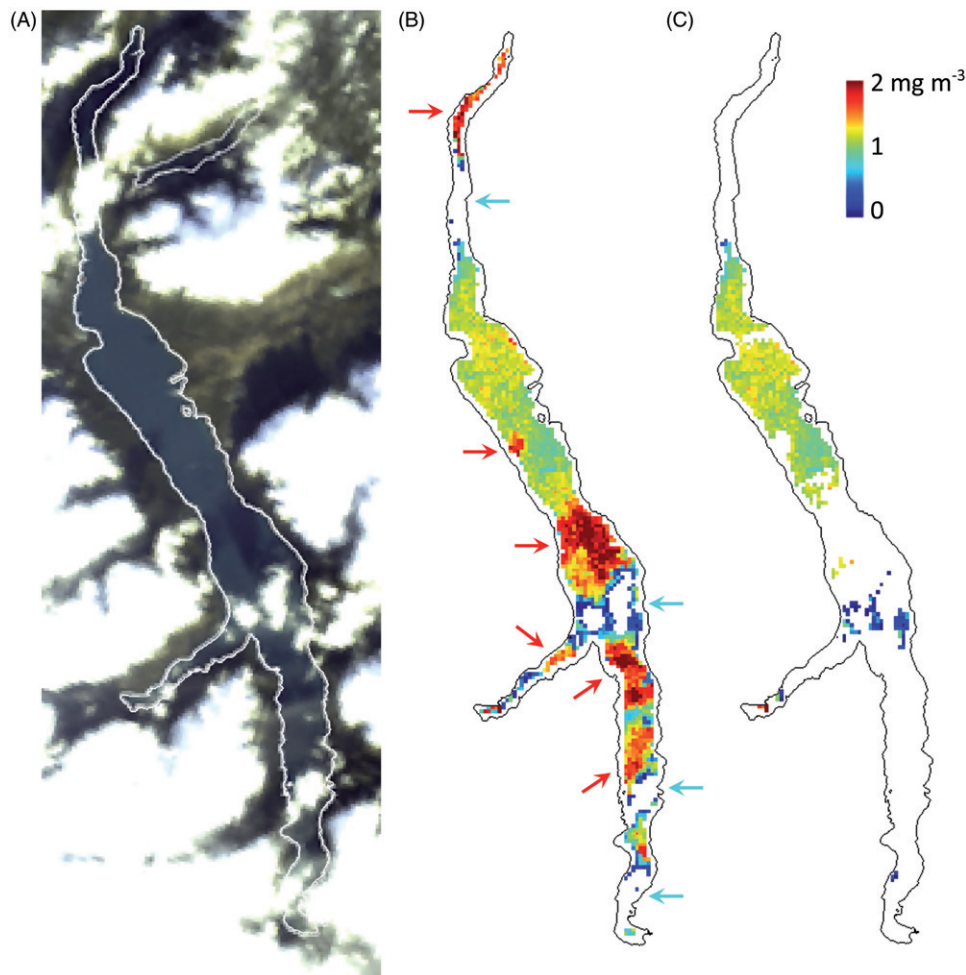


Figure 3. MERIS image from January 24, 2005, showing the amplifying effect of shadow on chlorophyll estimates. (A) L1 RGB; (B) C2R chlorophyll, showing elevated chlorophyll due to the presence of shadows (red arrows); (C) C2R chlorophyll with shadows masked based on a 560 nm reflectance threshold of 0.0012 sr⁻¹. Blue arrows in (B) indicate clouds masked by the Cloud Probability Processor.

as turbidity plumes. Algorithm performance was assessed on the basis of coefficient of determination (r^2) and Root Mean Square Error (RMSE) of the image retrievals relative to the *in situ* measurements of chlorophyll *a*.

Satellite chlorophyll time series

In addition to the cloud masking performed for the validation scenes (section 3.3.2), additional quality control steps applied to the C2R time series included land and shadow masking, low sun angle assessment, definition of valid pixel coverage, model goodness-of-fit assessment, and visual assessment for presence of haze, ice and smoke (Figure 2). Details for each quality control step are provided below.

Land masking. Two versions of a land mask were created from the shoreline polygon used to assess

navigation. The first, an inclusive mask intended primarily for image visualization was equivalent to the lake area as defined by the shoreline polygon, plus a one-pixel buffer around the periphery to show the shoreline and allow for slight navigation errors of individual scenes. The second, an exclusive mask intended for time series extractions was equivalent to the lake area, less a one-pixel buffer to exclude the possibility of contamination resulting from slight errors in image navigation and adjacency effects on the water reflectance. Adjacency refers to multiple scattering of light between the atmosphere and the surface, with the result that some light from outside the sensor field of view is scattered into the field of view of the sensor (e.g., Bulgarelli and Zibordi 2018). It is most apparent along boundaries with high contrast, as light from bright targets can be scattered so

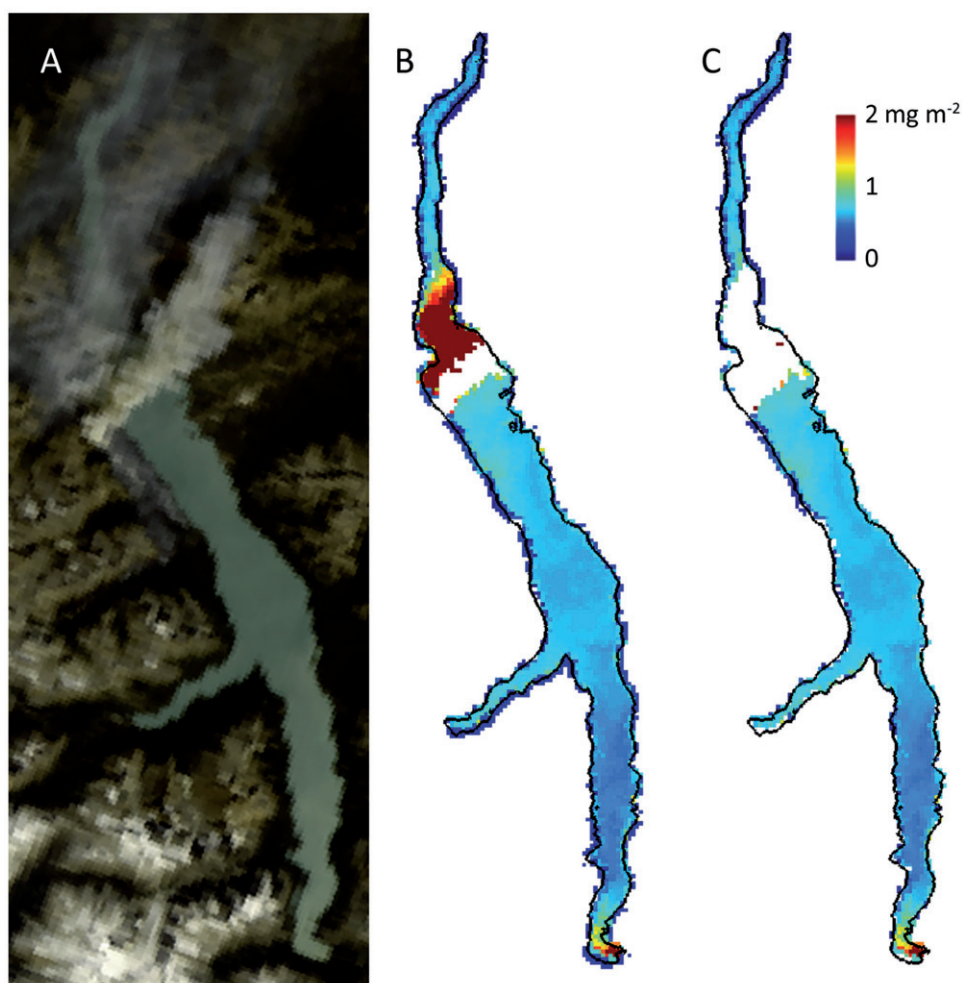


Figure 4. MERIS image from August 27, 2009, showing the presence of smoke and its effect on chlorophyll estimates. A. L1 RGB. B and C. C2R chlorophyll, before (B) and after (C) manual smoke masking.

as to contaminate the signal from dark water pixels, reducing the contrast and in the case of water, interfering with derivation of in-water constituents.

Shadow masking. Cloud shadow has the effect of depressing apparent reflectance and increasing apparent chlorophyll (Werdell et al. 2010). This is demonstrated in Figure 3. The C2R neural net algorithm is not run when water leaving remote-sensing reflectance is less than $1.3 \times 10^{-7} \text{ sr}^{-1}$ in 5 or more of the 8 spectral channels used (Doerffer and Schiller 2007), but in practice we found that this extremely low threshold did not remove chlorophyll artifacts due to shadow. In comparison, for SeaWiFS a shadow flag is set based on water-leaving radiance at 555 nm (Patt et al. 2003). Following this example, we therefore selected the 560 nm MERIS band as the basis for shadow masking. The reflectance of pure water at this wavelength is 0.0013 sr^{-1} (Morel and Prieur 1977). The presence of phytoplankton or mineral particles would tend to

increase reflectance in this range due to light scattering, and spectral absorption at 560 nm by phytoplankton pigments or dissolved organic matter should be relatively small (Morel and Prieur 1977), so we selected a threshold of 0.0012 sr^{-1} for shadow detection. Visual inspection and experimentation with thresholds between 0.0010 – 0.0015 sr^{-1} suggested that this threshold was appropriate (e.g., Figure 3C).

Low sun angle. In addition to shadow masking, scenes acquired at low sun elevation of less than 15 degrees were removed from the time series, consistent with standard processing for MODIS and SeaWiFS (Wang 2002). At the latitude of Chilko Lake, this included all scenes acquired between December 4 and January 13 of each year.

Model goodness-of-fit. As a check for model goodness-of-fit the C2R algorithm generates a χ^2 statistic that compares, on a pixel-by-pixel basis, the agreement between measured reflectance and that predicted

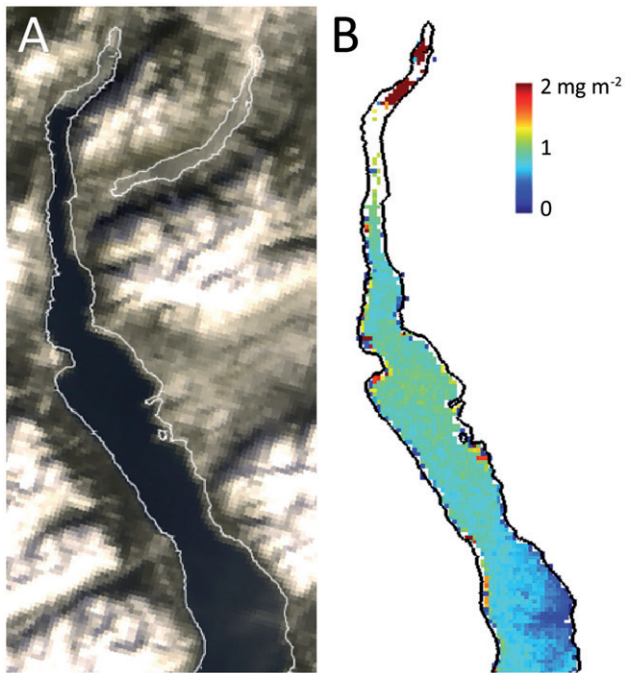


Figure 5. March 5, 2008 MERIS image with ice at the north end of Chilko Lake. A. L1 RGB. B. C2R chlorophyll after masking for cloud, shadow and χ^2 , showing elevated chlorophyll in the north part of the lake where the surface water is ice covered.

by the optical model (Doerffer and Schiller 2007). χ^2 is calculated as

$$\chi^2 = \sum (\ln(RL_w meas) - \ln(RL_w fNN))^2$$

where $RL_w meas$ is the observed MERIS reflectance, $RL_w fNN$ is the reflectance predicted by the optical model for the estimated combination of chlorophyll, SPM and CDOM concentrations, and χ^2 is the squared differences of the natural log transformed reflectance, summed over the 8 spectral bands (between 412 and 708 nm) used in the model (Doerffer and Schiller 2007). The C2R processor sets an out-of-scope flag if χ^2 exceeds 4.0 (corresponding to an average spectral ratio between measured and modeled reflectance of 2.0). In spot checks we found that this flag was rarely set. We examined time series of χ^2 and found that model performance was generally worst (highest χ^2) in winter scenes when the sun angle marginally exceeded the critical value of 15 degrees. To be conservative, we reduced the χ^2 threshold for poor model fit to a value of 1.0, corresponding to an average spectral ratio of 1.4. This produced expected results; i.e., reduced mean chlorophyll estimates during winter in some years.

Valid pixel coverage and visual assessment. Some images were heavily impacted by the application of masking for clouds, shadows and model fit, and as a

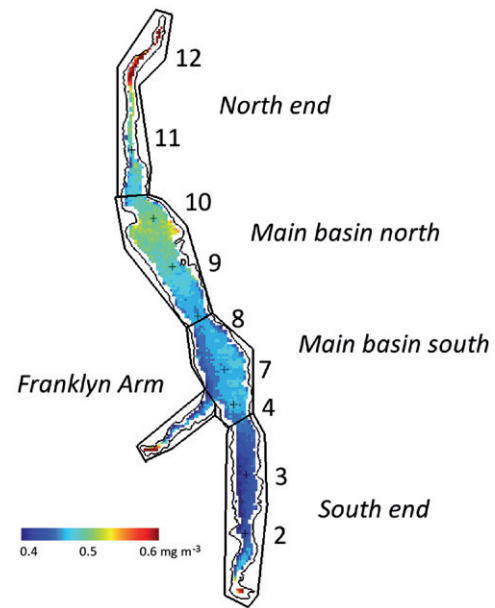


Figure 6. Five sub-regions from which time series were extracted, with locations of field sampling stations. The background image is the overall 2002-2012 February to November mean chlorophyll concentration, calculated as the mean of monthly climatologies. Note that this colour scale is different from others in the text.

Table 2. Summary of chlorophyll algorithm validation, based on comparisons with our *in situ* surface chlorophyll. P = statistical probability based on the F-statistic, RMSE = root mean square error in mg m^{-3} .

| | C2RB v1.4.1 | C2RB v1.0.2 | C2R v1.4.1 | C2R v1.3.2 | FUB/WeW |
|----------------|-------------|-------------|------------|------------|------------|
| N | 95 | 95 | 95 | 95 | 95 |
| R ² | 0.37 | 0.48 | 0.48 | 0.55 | 0.12 |
| P | 0.000 | 0.000 | 0.000 | 0.000 | 0.001 |
| RMSE | 0.74 (123%) | 0.49 (105%) | 0.44 (74%) | 0.27 (45%) | 0.39 (65%) |

result few valid pixels remained for these images. On the basis that these affected images represented data acquired under marginal conditions, and that the remaining non-masked pixels could be of low quality – for example, subject to thin cloud not flagged by the Cloud Probability Processor – images with less than 10% pixels corresponding to lake coverage were excluded from the time series. Finally, the remaining scenes were visually assessed for artifacts. For instance, one scene affected by a forest fire was masked to remove pixels with elevated chlorophyll due to the presence of smoke (note in Figure 4 the overestimation of chlorophyll in the smoke plume which had been only partially masked using other quality control measures).

Ice mask. The surface of Chilko Lake occasionally freezes in its narrow north arm. Ice was not reliably detected by any of the masking algorithms previously

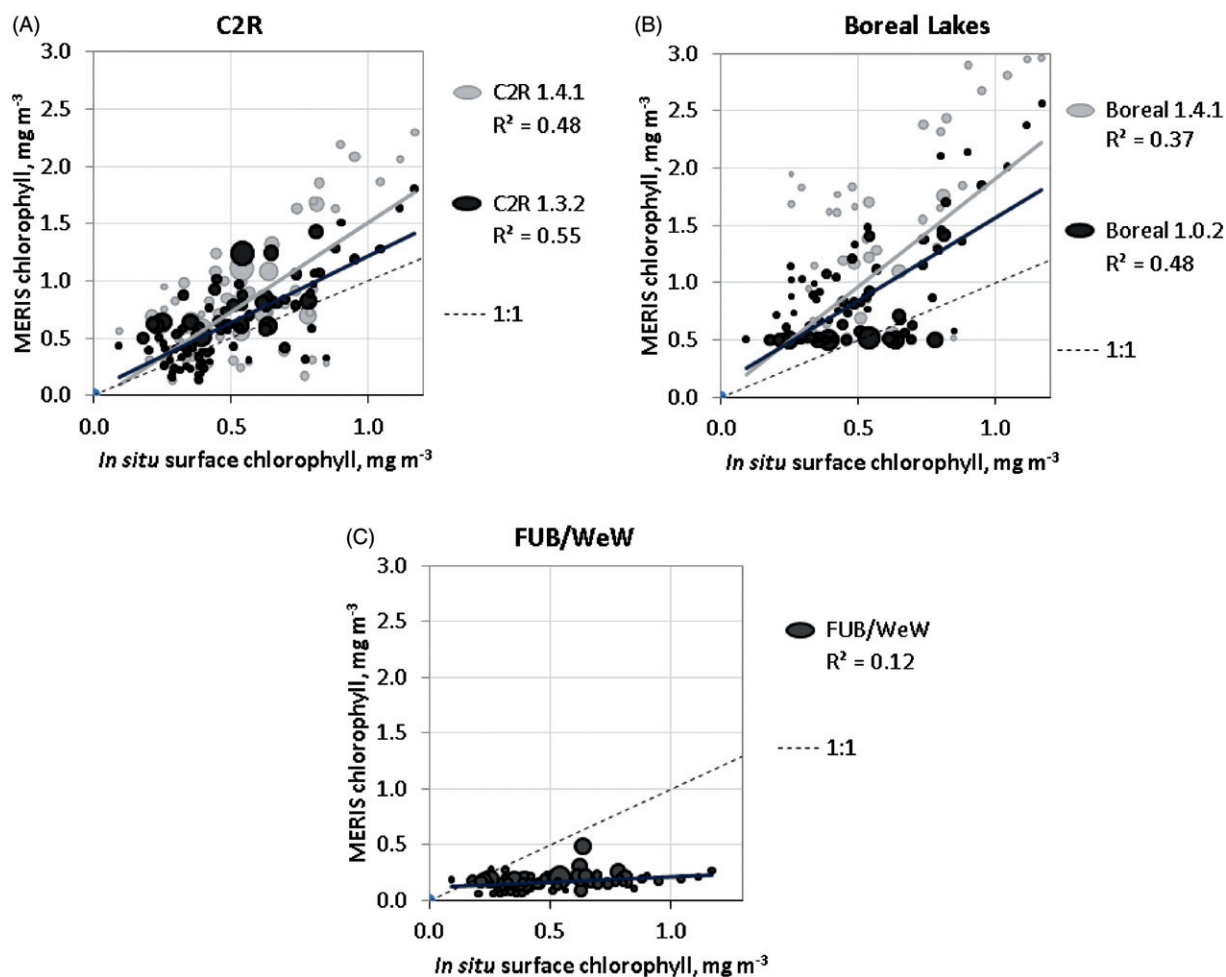


Figure 7. Validation scatterplots for the three MERIS chlorophyll algorithms evaluated, relative to field measurements of surface chlorophyll. Symbol size is proportional to turbidity between 0.07 and 3.3 NTU. A. C2R. B. Boreal lakes. C. FUB/WeW.

applied in the processing chain, but when present falsely elevated chlorophyll estimates (Figure 5). To correct for the possible presence of ice, a mask of affected pixels was defined manually for all scenes acquired between November 1 and April 30 of each year.

Temporal binning, spatial averaging and phenology calculations. Following the quality control steps, the final chlorophyll time series consisted of 996 scenes acquired between June 18, 2002 and April 5, 2012. These were binned into 8-day and monthly composites by averaging valid pixel values for each binned period. To characterize the annual cycle, 8-day and monthly climatologies were calculated as the means across years. For interpretation, area averaged time series were extracted from five sub-regions (chosen based on the limnology of the lake) as defined in Figure 6, as well as a whole lake average. For each sub region a smoothed (canonical) annual cycle was fitted, using least squares criteria, to the

extracted 8-day time series as the sum of three sinusoids with fixed periods of 1.0, 0.5, and 0.33 years, according to the methods of Jackson et al. (2015). Spectral analysis revealed that these periods, originally derived for coastal chlorophyll time series, were also appropriate for Chilko Lake, with the 1.0 and 0.5 year harmonics being the two dominant components present in all defined regions, and the 0.33 year harmonic more weakly defined and variable among regions.

For each sub region, the timing of annual bloom initiation and peak were calculated from 8-day and monthly time series, respectively. Bloom initiation was determined using the algorithm of Siegel et al. (2002), which defines the beginning of the bloom as the year-day when chlorophyll levels first raise a small threshold (5%) above the annual median. In our application of the algorithm we used a biological year beginning at the minimum of the canonical cycle, rather than a

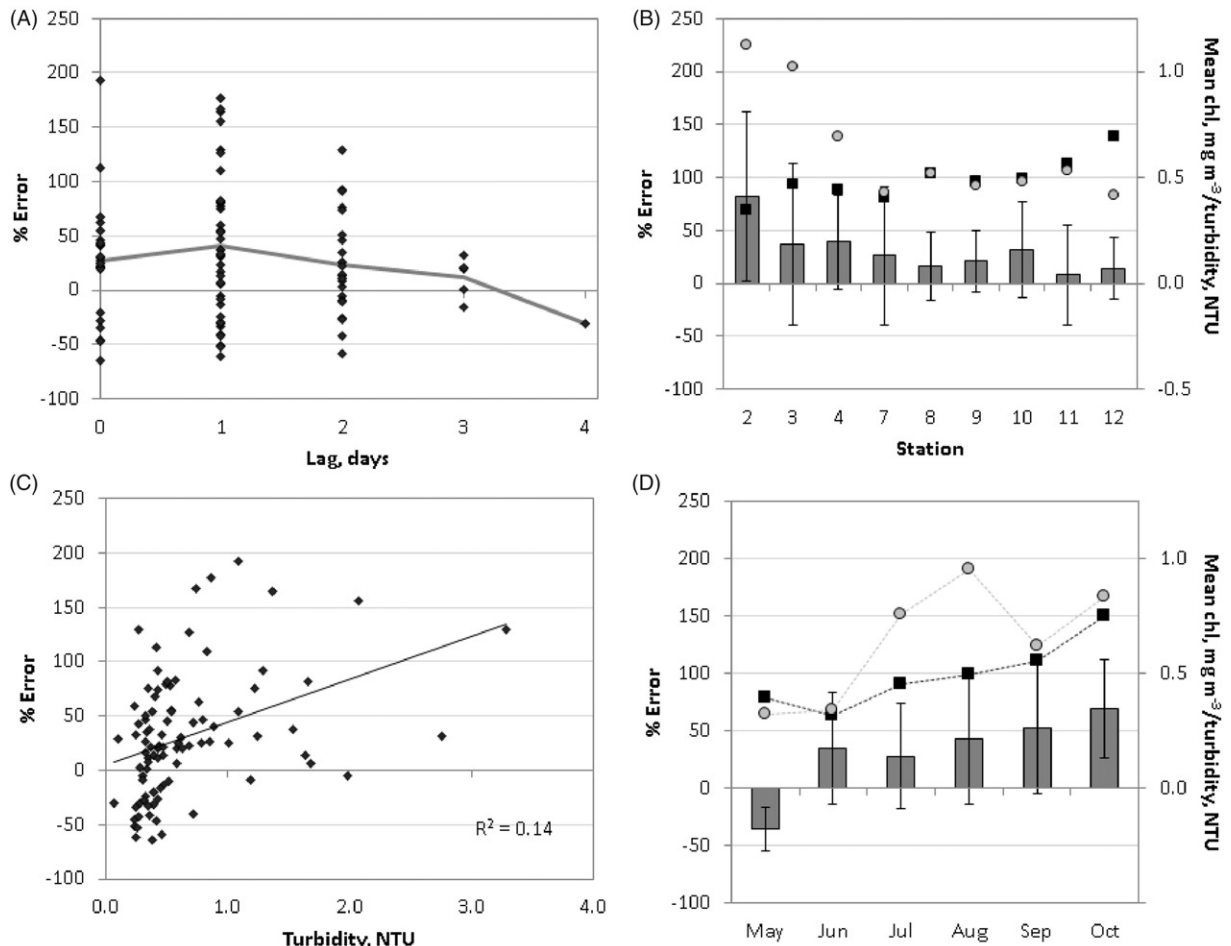


Figure 8. Relationship between residuals (expressed as percentage error) in C2R 1.3.2 chlorophyll estimates and (A) data acquisition match-up differences, (B) location, (C) turbidity, and (D) month. In (B and D), mean *in situ* concentration for each station (chlorophyll, black squares; turbidity, grey circles) is compared to the mean residual (wide bars) and the range of error.

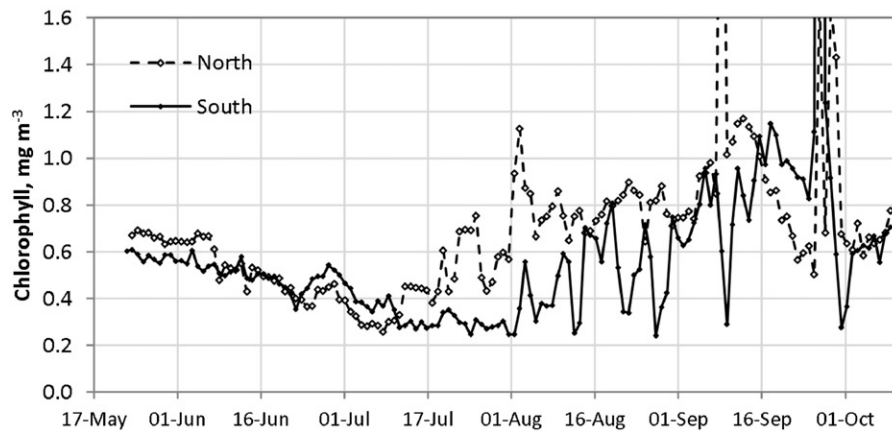


Figure 9. Time series of mean daily chlorophyll estimated from night-time fluorescence (so as to avoid day time photo-inhibition) from two fluorometers moored in Chilko Lake during 2012. In this plot the Y scale has been expanded to show day-to-day variability; maximum values off the plot were Sept 9: 3.1 (North) and Sept 27: 12.7 (South), 1.7 (North); Sept 29: 1.7 (North).

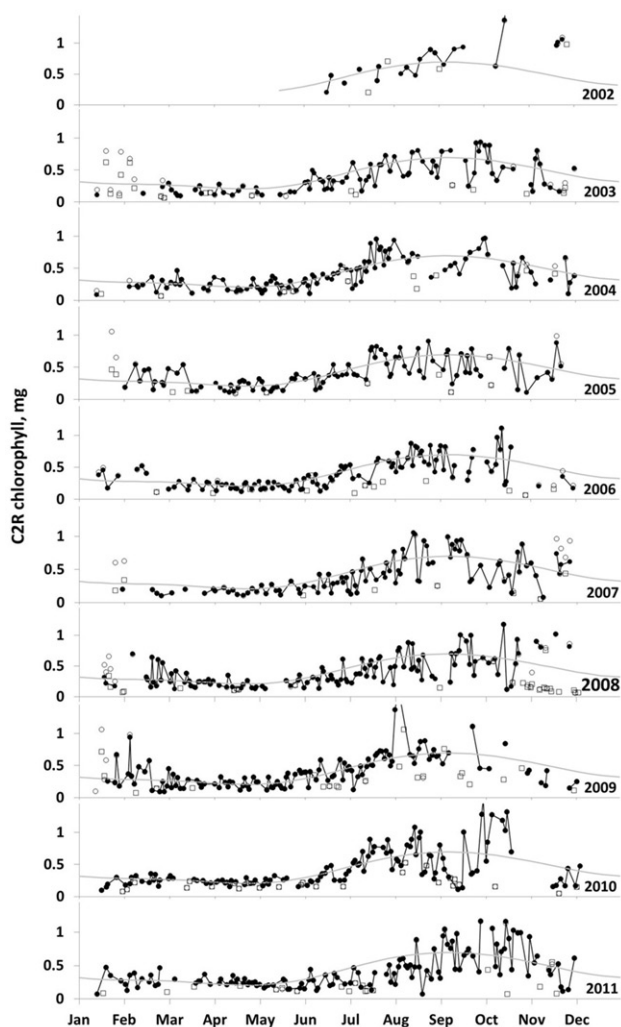


Figure 10. Daily time series of MERIS C2R 1.3.2 chlorophyll averaged over the whole lake. Open symbols show points that were shifted due to masking of pixels for model goodness-of-fit (circles) or removed due to low spatial coverage (squares). The final time series is shown by the solid symbols and a black line joining points less than 7 days apart. The grey line gives the canonical annual cycle, calculated as the least squares best fit sum of three sinusoids with fixed periods of 1.0, 0.5, and 0.33 years.

calendar year. Peak chlorophyll timing was determined from the monthly time series in order to remove the high-frequency variability present in the daily and 8-day time series.

Results

Algorithm performance

Table 2 summarizes the performance of the tested chlorophyll algorithms. Of the six variants, the best statistical results were obtained using the C2R algorithm version 1.3.2, with a coefficient of

determination of 0.55. Validation scatterplots (Figure 7A) show that C2R estimated chlorophyll reasonably well under a range of turbidity (indicated by symbol size), with a small positive bias, resulting in a lowest RMSE (0.27 mg m^{-3} or 45%). The version 1.4.1 of the algorithm overestimated chlorophyll at concentrations above about 0.7 mg m^{-3} , relative to version 1.3.2. The statistical results of C2RB (Figure 7B) were relatively similar, but overestimated (slope of 1.88) chlorophyll to a greater extent and was unable to generate accurate predictions under conditions of high turbidity. It also suffered from insufficient sensitivity, with a detection limit of 0.5 mg m^{-3} (Table 1). The FUB/WeW algorithm was poorly correlated with *in situ* chlorophyll concentration; consistently producing underestimates (Figure 7C).

Note that this study was carried out during 2012–2013. A recent paper by Seegers et al. 2018 recommends the use of other metrics based on simple deviations (e.g., bias, mean absolute error, pair-wise comparisons) “that often provide more robust and straightforward quantities for evaluating ocean color algorithms with non-Gaussian distributions and outliers.” Follow-on work to this study should consider these methods.

Sources of error

Sources of systematic “error” (defined here as differences between the concentrations measured in discrete 50 mL surface water samples and that derived for a 750 m area centered on that location from MERIS) in the C2R 1.3.2 chlorophyll estimates were examined, to aid in the interpretation of the predicted values. Figure 8 shows that there were weak relationships between error and station location, turbidity, and month, but not the time difference between image acquisition and field sampling (note that the ranges overlap, and that there was only one pairing at 4 days). For station location (Figure 8B), there was a slight north-south trend. The three highest turbidities at the south end of the lake, also have the highest average error. Stations 2 and 3 in the south end of the lake showed average turbidity values higher than 1.0 NTU compared to levels closer to 0.5 NTU at stations 4 to 10 in the central region and stations 11 and 12 in the north (grey circles). This is consistent with the turbidity relationships shown in Figure 8C. There was also a tendency to increased error later in the year when sun elevation decreased and wind speed and wave heights increased, with underestimates in May and overestimates in the other months. The increase

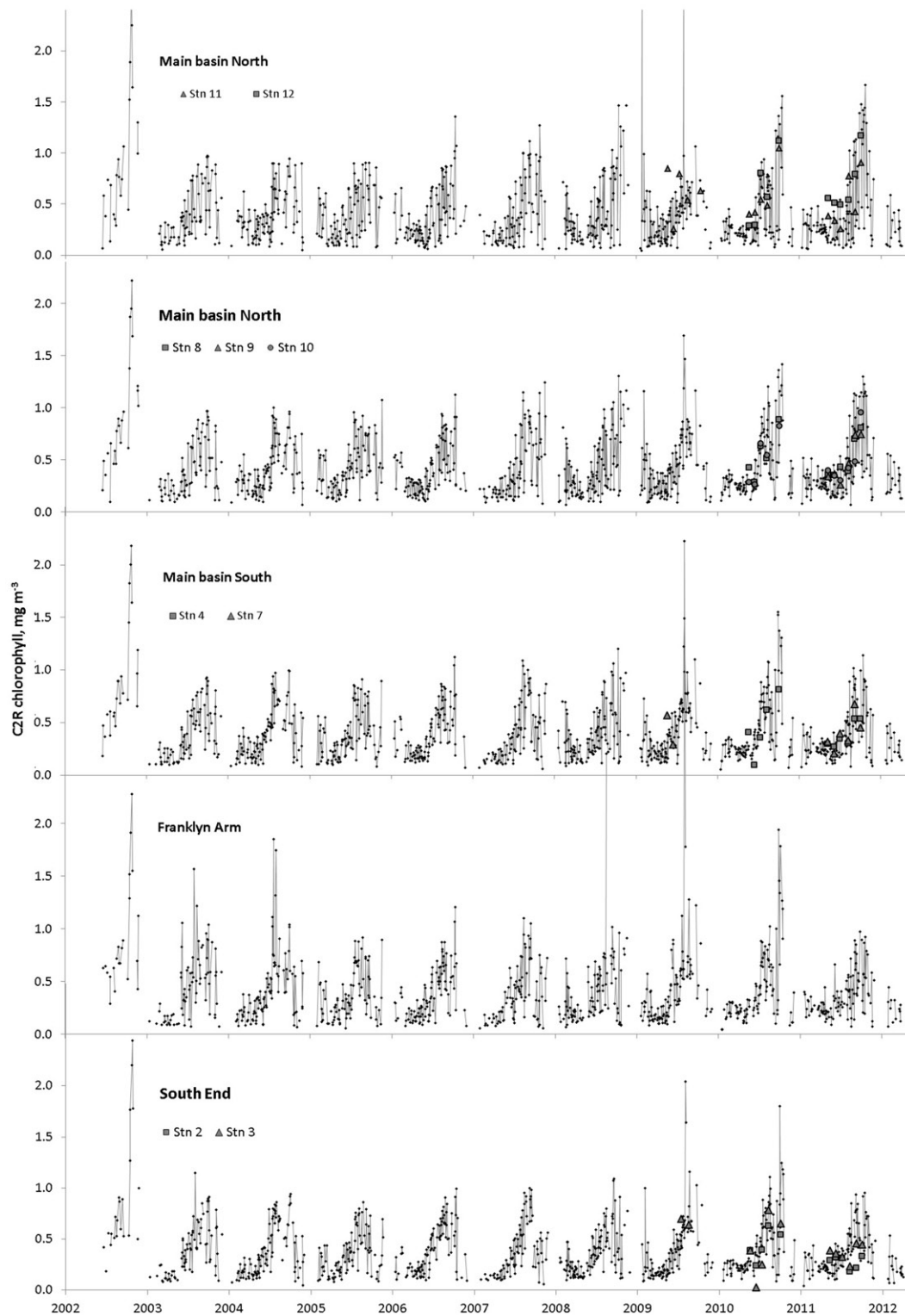


Figure 11. Daily MERIS chlorophyll time series for the five Chilkol Lake sub-regions, showing 2009–2011 field measurements for comparison. Legends for the station symbols are shown on each plot. No field measurements were available for Franklyn Arm.

in error during the fall months may also relate to the increased chlorophyll levels at that time of year, and the associated spatial variability. Although *in situ*

estimates of daily chlorophyll were not available for the time of the MERIS imagery, two fluorometers moored in the lake in 2012 clearly demonstrate

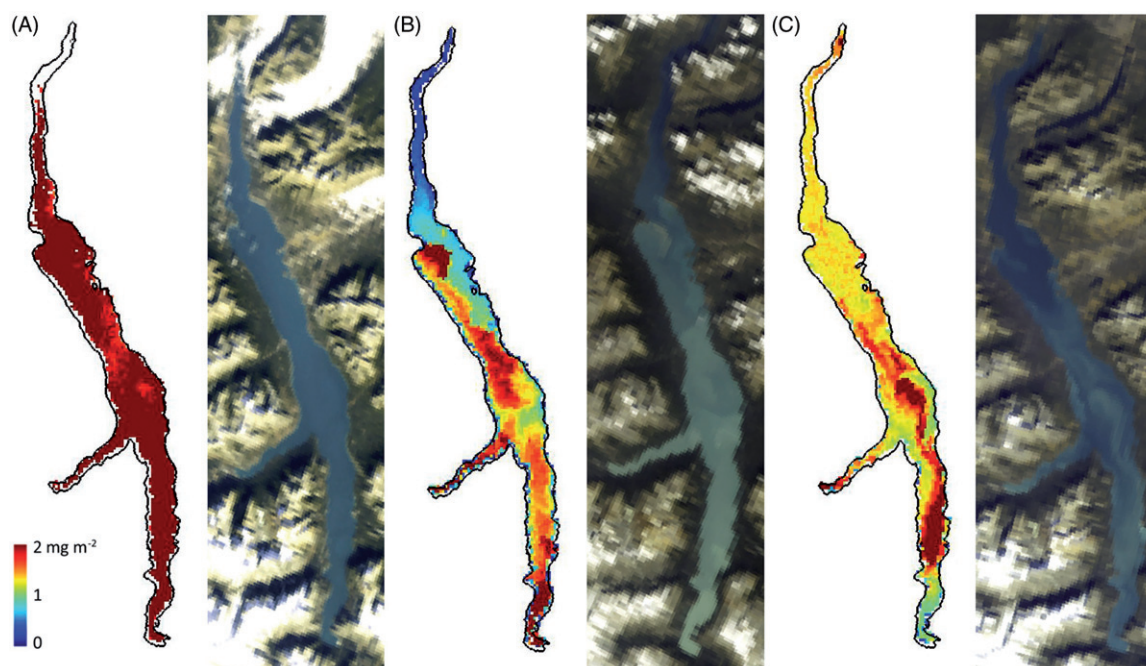


Figure 12. C2R chlorophyll and near true color MERIS images from dates of high chlorophyll events. A. October 26, 2002. B. August 6, 2009. C. September 30, 2010.

increased variability in conjunction with increased concentrations later in the year (Figure 9).

Chlorophyll time series

Figure 10 illustrates the evolution of the daily C2R chlorophyll time series for Chilko Lake as a whole, before masking for goodness of fit, and removing dates due to low (less than 10%) spatial coverage. As noted earlier, the greatest effect of masking for model fit was to reduce winter chlorophyll estimates, and the effect of removing scenes with low coverage was to remove many of the low chlorophyll values from the time series. The removal of low coverage scenes resulted in some long temporal gaps, but these occurred primarily during winter.

Daily chlorophyll time series for the lake sub-regions are shown in Figure 11. Field measurements made during 2009–2011 are overlaid to show the good agreement with the satellite estimates. All time series showed some day-to-day variability, with a consistent seasonal cycle corresponding to known dynamics: very low chlorophyll (less than $0.5\text{mg}/\text{m}^3$) between January and May with seasonal maxima near $1\text{mg}/\text{m}^3$ between August and November. However, occasional large spikes were observed, the largest of which occurred in October 2002, August 2009 and September 2010. Those in the latter 2 years might relate to large forest fires around the lake in 2009,

which provided increases in nutrient inputs from terrestrial runoff during from autumn rains. Imagery for those dates shows a relationship with turbidity (Figure 12). Although Figure 8C suggests that the spikes of elevated chlorophyll levels might be in part an artifact, the fluorometer data from 2012 suggest that these are likely real phenomena, associated with wind events, at least during September and October (Figure 13). There was considerable variation in *in situ* fluorescence on time scales less than an hour during these events (not shown), perhaps due to eddies and other small scale spatial heterogeneity that are generally not reflected in the satellite imagery. The shortest scale variability may be due to resuspension of algal mats or to the colonial cyanophyte *Synechococcus*. Stockner and Shortreed (1994) reported that it comprised about 99% of the autotrophic phytoplankton in the lake in the 1980s and 90s.

Climatologies: The 8-day climatology (for 2002 to 2012) and canonical cycles for the five sub-regions (Figure 14), and monthly climatology images (Figure 15) describe regional annual chlorophyll cycles with minima in April that rise to two peaks in the fall. There is some variability among sub regions, with the earliest (August) peak occurring in Franklyn Arm, and a trend toward later (October) and slightly higher maxima along a south-to-north gradient in the rest of the lake (Table 3). Because Lake Chilko is near the Coast Mountains it experiences frequent strong winds

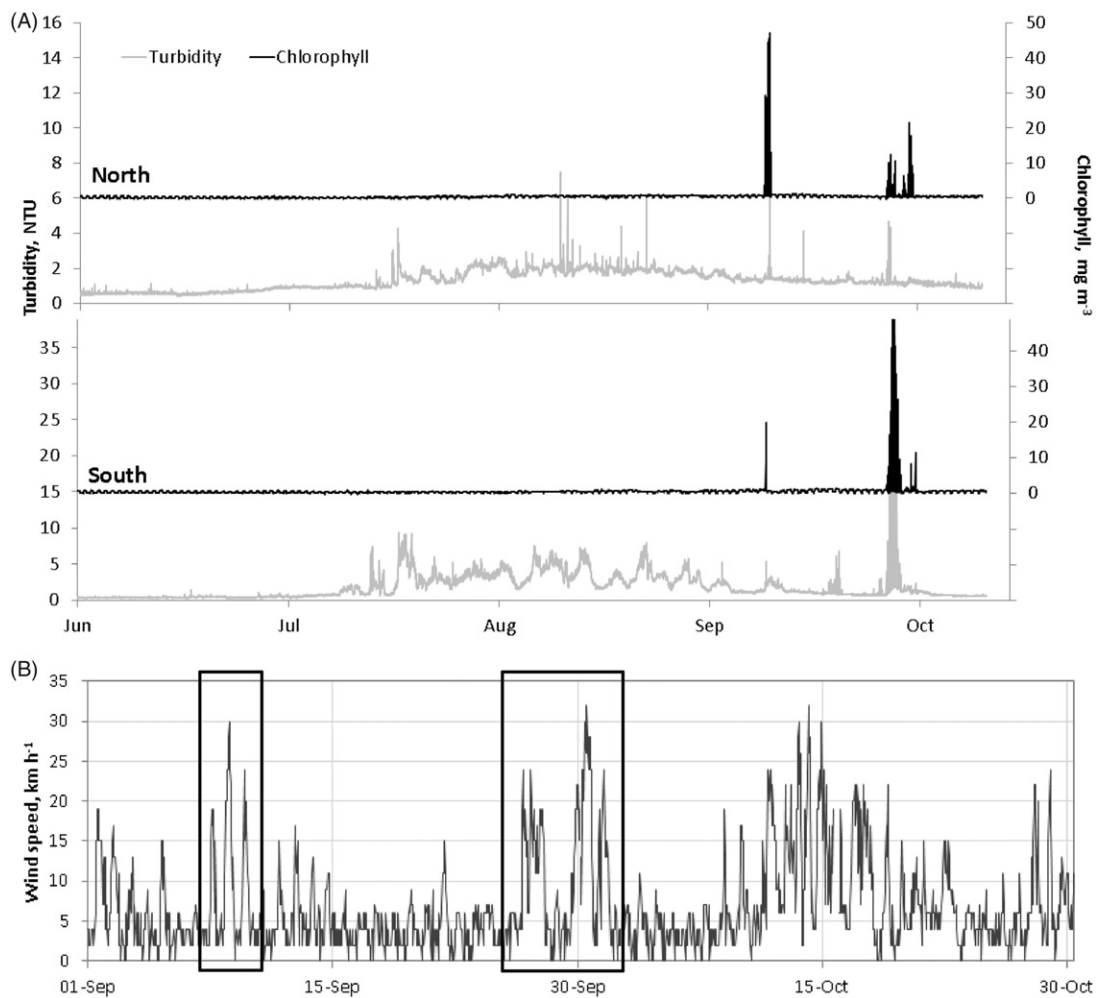


Figure 13. A. Comparison of chlorophyll (black) and turbidity (grey) time series from the two fluorometers moored in Chilko Lake in 2012. B. September and October wind speeds at Tatlayoko Lake, 15 km west of Chilko Lake (Environment Canada, 2012). Boxes show the dates of wind events on September 9–10 and September 27 to October 1 that corresponded to high chlorophyll fluorescence recorded in Chilko Lake.

along the axis of the lake, and has an unstable thermal regime (Grant et al. 2011). The lake is therefore isothermal much of the year with a deep, well-mixed epilimnion. What little stratification that does occur begins after the freshet in July, in the shallower clearer northern parts of the lake.

Figure 16 shows the interannual variability in the timing of the chlorophyll cycle in the sub-regions. Bloom initiation (Figure 16A) was variable among regions (up to 56 days' difference between Franklyn Arm and the two northernmost zones in 2008), but with the order (earliest to latest) consistent with the timing of the canonical cycles of the regions in most years. The year 2009 was an exception, with an early bloom start in all regions. The timing of peak chlorophyll at a monthly scale tended to be consistent among zones, although in some years (notably 2004) a north-south separation was present (Figure 16B). In

most sub-regions, 2008 was a distinctly late year. A limnological analysis of these differences as they relate to interannual differences in physical drivers such as winds, insolation and glacial runoff is outside the scope of this study.

Discussion

This study provides an evaluation of reflectance-based algorithms for chlorophyll *a* retrieval in a glacially influenced, ultra-oligotrophic case 2 lake system in British Columbia, Canada. At the time of this study (2011–2013), the European MERIS sensor on ENVISAT was the only space sensor providing chlorophyll imagery of suitable spatial resolution for Chilko and other large BC lakes. The analysis initially considered 1425 scenes with at least partial cloud-free coverage of the lake for the period June 18, 2002–April 6,

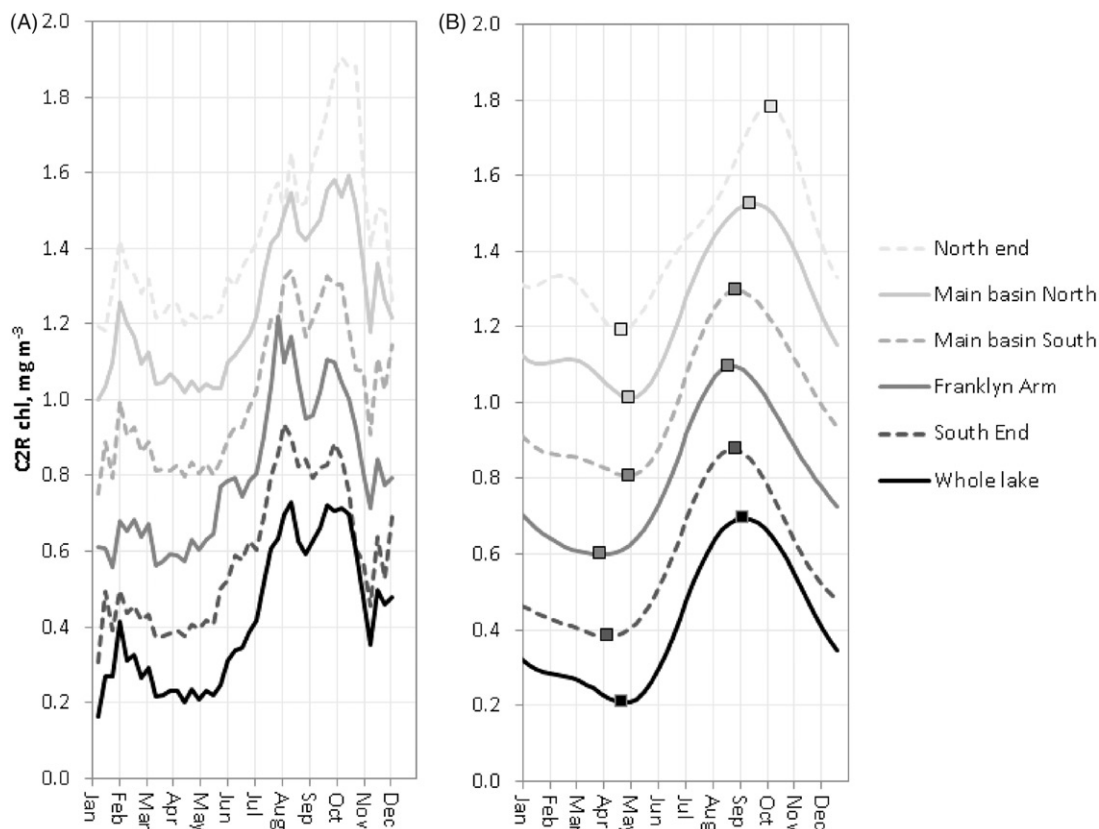


Figure 14. 8-day chlorophyll climatology (A), and canonical cycles for Chilko Lake and its sub-regions (B). The maxima and minima of the canonical cycles are marked by square symbols. In both figures, the Y-scales apply to the whole lake data series (black). Plots for the sub-regions are offset by 0.2 mg m⁻³.

2012. For this data set, considerable pre-processing and manual inspection was required to produce a high-quality dataset. Corrections to image navigation, masking for cloud, smoke, shadow, ice and low sun elevations were required.

Comparison with historical *in situ* chlorophyll data obtained by standard methods was possible for 16 matching scenes and 98 validation points acquired within 4 days of image acquisition. Although regional chlorophyll algorithms have not yet been developed for Chilko Lake or other British Columbia lakes, we found that at least one standard ESA algorithm developed elsewhere performed well. The C2R algorithm produced for ESA was trained on mostly coastal European waters, with a wide range of chlorophyll and turbidity (Doerffer and Schiller 2007). In spite of this, comparison with *in situ* chlorophyll measurements was generally good – both in magnitude and temporal and spatial variability – with errors associated with inorganic turbidity likely resulting from wind events in the fall. This occurs mostly in the south nearest the glaciers.

The C2R image-time series show considerable short-term variability, which appears to be a real

effect of strong wind events that are well known on Chilko Lake. Regional differences in chlorophyll timing were verified by field data. Interannual differences in chlorophyll abundance and timing, which may be important determinants of salmon growth and production, were well described.

Chilko Lake is a twelve hour drive from the DFO laboratory near Vancouver responsible for most Fraser River watershed limnological sampling; hence the expense of sampling limits the frequency of visits. Moreover, there are more than 20,000 lakes in British Columbia and hundreds of thousands across the north, most of which are remote and accessible only by float plane or helicopter. Primary production or even chlorophyll concentration has not been measured for most. Where *in situ* data do exist they are sporadic and time series are short. By contrast, satellite sensors of many types now provide wide area global coverage and growing time series. Although MERIS ceased operation in April 2012 after 10 years in service, it has been replaced by the OLCI (Ocean and Land Color Instruments) on the European SENTINEL 3a and 3b satellites launched in February 2016 and April 2018, respectively.

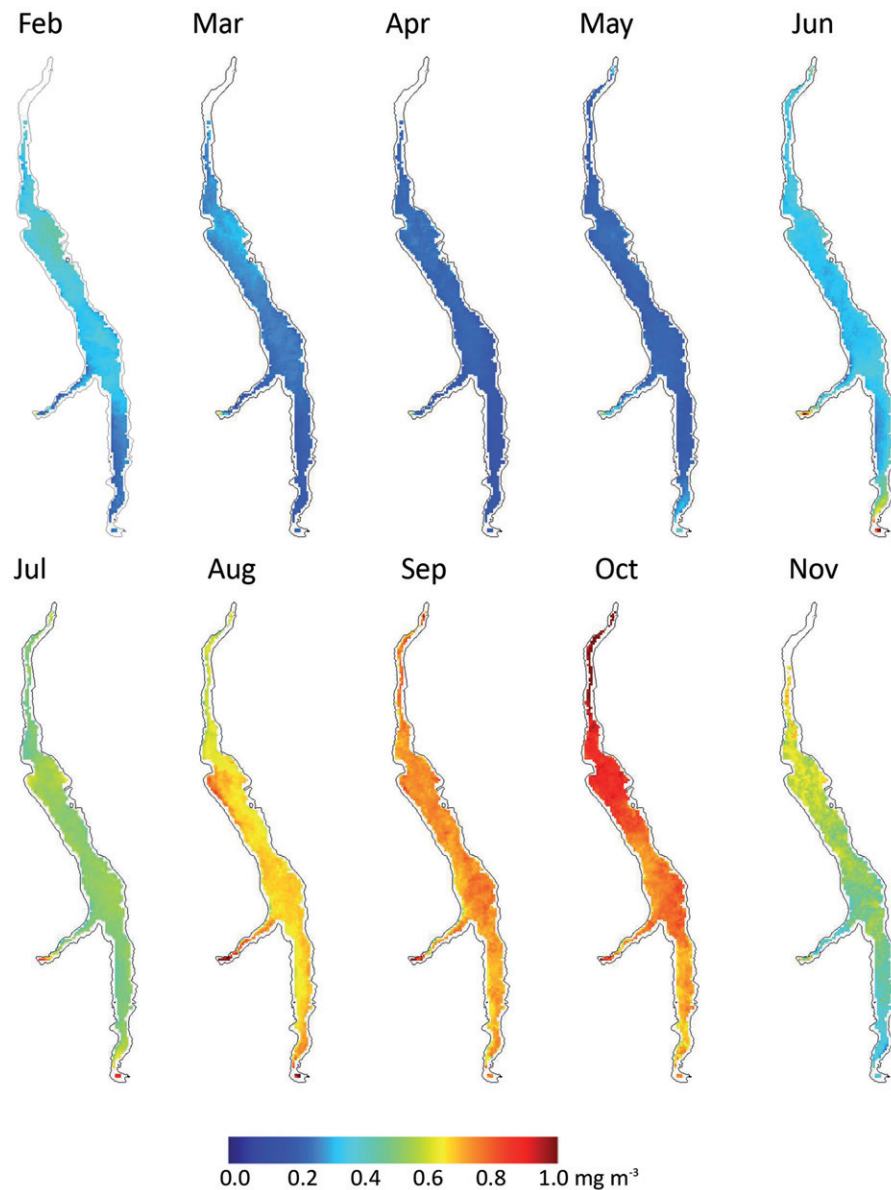


Figure 15. Monthly C2R chlorophyll climatology for Chilko Lake. The northern tip of the lake is masked during months with ice (November to April). December and January are excluded due to low sun angle during most of this period.

Table 3. Summary of minima and maxima of the canonical chlorophyll cycles in Chilko Lake and its five sub-regions.

| Sub-region | Julian day | Min date | Chl | Julian day | Max date | Chl |
|------------------|------------|----------|------|------------|----------|------|
| North end | 113 | 23 Apr | 0.19 | 281 | 08 Oct | 0.78 |
| Main basin north | 121 | 01 May | 0.21 | 257 | 14 Sep | 0.73 |
| Main basin south | 121 | 01 May | 0.21 | 241 | 29 Aug | 0.70 |
| Franklyn Arm | 89 | 30 Mar | 0.20 | 233 | 21 Aug | 0.70 |
| South end | 97 | 07 Apr | 0.18 | 241 | 29 Aug | 0.68 |
| Whole lake | 113 | 23 Apr | 0.21 | 249 | 06 Sep | 0.70 |

Satellite derived estimates of chlorophyll *a* in sockeye salmon rearing lakes have significant potential as a fisheries planning and analysis tool. This study has demonstrated that satellite time series can provide reasonable estimates of chlorophyll *a*, novel phenological

information and quasi-continuous data series in northern lakes, although periodic *in situ* verification are necessary. Chlorophyll *a*, as a surrogate measure for primary production, typically correlates with zooplankton biomass, the freshwater forage for young sockeye salmon in nursery lakes (Hume et al. 1996). Thus, elevated primary production can lead to improved freshwater growth and survival, influencing adult salmon returns 2 years later (Hyatt et al. 2004). Being better able to anticipate good and poor returns 2 years ahead would be a significant benefit to fishery managers. We encourage further collaborative studies that include both remote-sensing experts and potential users of this technology including limnologists and fisheries biologists.

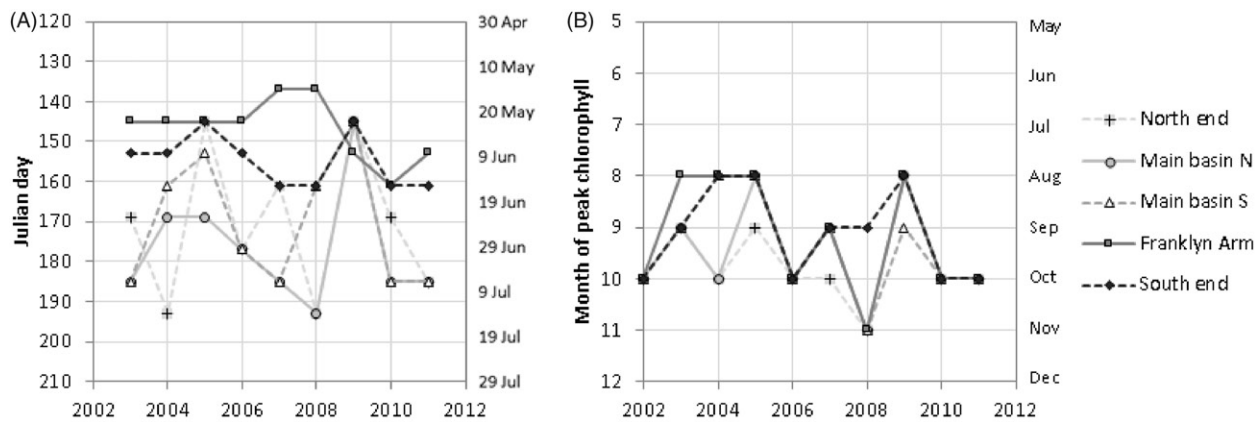


Figure 16. Timing of bloom initiation (A), and timing of peak chlorophyll (B), for the five Chilko Lake sub regions.

Disclosure statement

No potential conflict of interest was reported by the authors.

Funding

Funding for this study was provided by the Earth Observations Applications Development Program (EOADP) of the Canadian Space Agency (CSA), Fisheries and Oceans Canada and ASL Environmental Sciences Inc. Excellent technical assistance was provided by Randy Kerr and Peter Willis of ASL.

References

- Akenhead, S.A., Irvine, J.R., Hyatt, K.D., Johnson, S.C., Grant, S.C.H., and Michielsens, C.G.J. 2016. "Habitat manipulations confound the interpretation of sockeye salmon recruitment patterns at Chilko Lake, British Columbia." *North Pacific Anadromous Fish Commission Bulletin*, Vol. 6: pp. 391–414. doi:10.23849/npafcb6/391.
- American Public Health Association. 1998. "Turbidity (2130)." In *Standard Methods for the Examination of Water and Wastewater*, edited by L. S. Clesceri, A. E. Greenberg, and A. D. Eaton. 20th ed. Baltimore MD: United Book Press.
- Babin, M. 2000. "Coastal surveillance through observation of ocean color (COASTLOOC)." Final Report, Project ENV4-CT96-0310, 233 p. Laboratoire de Physique et Chimie Marines, Villefranche-sur-mer, France.
- Bricaud, A., Morel, A., Babin, M., Allali, K., and Claustre, H. 1998. "Variations of light absorption by suspended particles with chlorophyll a concentration in oceanic (Case 1) waters: Analysis and implications for bio optical models." *Journal of Geophysical Research: Oceans*, Vol. 103 (NO. C13): pp. 31033–31044. doi:10.1029/98JC02712.
- Brockmann Consult. 2015. "Case 2 Regional Processor change log." <http://www.brockmann-consult.de/beam-jira/browse/CIIR/component/10161#selectedTab=com.atlassian.jira.plugin.system.project.component-changelog-panel&allVersions=true>
- Brockmann, C., and Doerffer, R. 2016. Evolution of the C2RCC neural network for Sentinel 2 and 3 for the retrieval of ocean colour products in normal and extreme optically complex waters. *Proc. Living Planet Symposium*, ESA SP-470
- Bulgarelli, B., and Zibordi, G. 2018. "Seasonal impact of adjacency effects on ocean color radiometry at the AAOT validation site." *IEEE Geoscience and Remote Sensing Letters*, Vol. 15 (No. 4): pp. 488–492. doi:10.1109/LGRS.2017.2781900.
- Doerffer, R., and Schiller, H. 2007. "The MERIS Case 2 water algorithm." *International Journal of Remote Sensing*, Vol. 28 (No. 3–4): pp. 517–535. doi:10.1080/01431160600821127.
- Doerffer, R., Schiller, H. 2008. *MERIS algorithm theoretical basis document (ATBD) MERIS Lake Water Algorithm for BEAM-V1.0*, 10 June 2008. Geesthacht, Germany: GKSS Research Center. www.brockmann-consult.de/beam-wiki/.../ATBD_lake_water_RD20080610.pdf.
- Environment Canada. 2012. http://climate.weather.gc.ca/climateData/hourlydata_e.html?timeframe=1&Prov=BC&StationID=30494&hlyRange=2000-08-10%7C2013-12-15&cmdB1=Go&Year=2012&Month=10&Day=30&cmdB1=Go#
- Fell, F., and Fischer, J. 2001. "Numerical simulation of the light field in the atmosphere-ocean system using the matrix-operator method." *Journal of Quantitative Spectroscopy and Radiative Transfer*, Vol. 69 (No. 3): pp. 351–388. doi:10.1016/S0022-4073(00)00089-3.
- Fischer, J., and Grassl, H. 1984. "Radiative transfer in an atmosphere-ocean system: an azimuthally dependent matrix-operator approach." *Applied Optics*, Vol. 23 (No. 7): pp. 1032–1039. doi:10.1364/AO.23.001032.
- Fomferra, N., and Brockmann, C. 2005. "BEAM - the ENVISAT MERIS and AATSR toolbox." MERIS (A) ATSR Workshop, Frascati, Italy. <http://articles.adsabs.harvard.edu/full/2005ESASP.597E..13F/0000013.001.html>.
- Gallie, E.A., and Murtha, P.A. 1992. "Specific absorption and backscattering spectra for suspended minerals and chlorophyll-a in Chilko lake, British Columbia." *Remote Sensing of Environment*, Vol. 39 (No. 2): pp. 103–118. doi:10.1016/0034-4257(92)90130-C.
- GeoBC. 2008. Freshwater Atlas Lakes – custom download. Website accessed October, 2018 at https://catalogue.data.gov.bc.ca/dataset/freshwater-atlas-lakes/resource/9595d129-03cc-40bb-b216-6ce3a1337143?inner_span=True

- Grant, S.C.H., MacDonald, B.L., Cone, T.E., Holt, C.A., Cass, A., Porszt, E.J., Hume, J.M.B., and Pon, L.B. 2011. "Evaluation of uncertainty in Fraser Sockeye WSP Status using abundance and trends in abundance metrics." *Canadian Science Advisory Secretariat*, pp. 183. Available at <https://www.psf.ca/sites/default/files/344553.pdf>.
- Hume, J.M.B., Shortreed, K.S., and Morton, K.F. 1996. "Juvenile sockeye rearing capacity of three lakes in the Fraser River system." *Canadian Journal of Fisheries and Aquatic Sciences*, Vol. 53 (No. 4): pp. 719–733. doi:10.1139/f95-237.
- Hyatt, K.D., McQueen, D.J., Shortreed, K.S., and Rankin, D.P. 2004. "Sockeye salmon (*Oncorhynchus nerka*) nursery lake fertilization: Review and summary of results." *Environmental Reviews*, Vol. 12 (No. 3): pp. 133–162. doi:10.1139/a04-008.
- Jackson, J.M., Thomson, R.E., Brown, L.N., Willis, P.G., and Borstad, G.A. 2015. "Satellite chlorophyll off the British Columbia Coast, 1997–2010." *Journal of Geophysical Research: Oceans*, Vol. 120 (No. 7): pp. 4709–4728. doi:10.1002/2014JC010496.
- Koponen, S., Ruiz Verdu, A., Heege, T., Heblinski, J., Sorensen, K., Kallio, K., Pyh  lahti, T., Doerffer, R., Brockmann, C., and Peters, M. 2008. "Development of MERIS lake water algorithms: Validation report". Helsinki, Finland: Helsinki University of Technology Version 1.01. https://www.brockmann-consult.de/beam-wiki/download/attachments/8355860/MERIS_LAKES_Validation_report.pdf
- Mobley, C. D. 1994. *Light and Water Radiative Transfer in Natural Waters*. New York: Academic Press, Inc. <http://www.oceanopticsbook.info/view/references/publications>.
- Morel, A., and Prieur, L. 1977. "Analysis of variations in ocean color." *Limnology and Oceanography*, Vol. 22 (No. 4): pp. 709–722. doi:10.4319/lo.1977.22.4.0709.
- Nidle, B.H., Shortreed, K.S., Masuda, K.V., Whitehouse, T.R., and Carrier, R.C. 1990. "Results of limnological investigations carried out in 1986 on 5 coastal and interior lakes in British Columbia." *Canadian Data Report of Fisheries and Aquatic Sciences*, Vol. 806: pp. 213. <http://publications.gc.ca/pub?id=9.577000&sl=0>.
- Odermatt, D., Giardino, C., and Heege, T. 2010. "Chlorophyll retrieval with MERIS Case-2-regional in perialpine lakes." *Remote Sensing of Environment*, Vol. 114 (No. 3): pp. 607–617. doi:10.1016/j.rse.2009.10.016.
- Odermatt, D., Gitelson, A., Brando, V.E., and Schaepman, M. 2012. "Review of constituent retrieval in optically deep and complex waters from satellite imagery." *Remote Sensing of Environment*, Vol. 118: pp. 116–126. doi:10.1016/j.rse.2011.11.013.
- Palmer, S.C.J., Hunter, P.D., Lankester, T., Hubbard, S., Spyarakos, E., Tyler, A.N., Pr  sing, M., et al. 2014. "Validation of Envisat MERIS algorithms for chlorophyll retrieval in a large, turbid and optically-complex shallow lake." *Remote Sensing of Environment*, Vol. 157 (No. 2015): pp. 158–169. doi:10.1016/j.rse.2014.07.024.
- Palmer, S.C.J., Odermatt, D., Hunter, P.D., Brockmann, C., Pr  sing, M., Balzter, H., and T  th, V.R. 2015. "Satellite remote sensing of phytoplankton phenology in Lake Balaton using 10 years of MERIS observations." *Remote Sensing of Environment*, Vol. 158: pp. 441–452. doi:10.1016/j.rse.2014.11.021.
- Patt, F. S., Barnes, R. A., Eplee, R. E. Jr., Franz, B. A., Robinson, W. D., Feldman, G. C., Bailey, S. W., et al. 2003. "Algorithm updates for the fourth SeaWiFS data reprocessing". In: Hooker, S. B. and E. R. Firestone (eds.), *SeaWiFS Postlaunch Technical Report Series*, Vol. 22. NASA Technical Memorandum 2003-206892. https://oceancolor.gsfc.nasa.gov/SeaWiFS/TECH_REPORTS/PLVol22.pdf.
- Preusker, R., Huenerbein, A., and Fischer, J. 2006. "Cloud detection with MERIS using oxygen absorption measurements." *Geophysical Research Abstracts*, Vol. 8: pp. 09956. https://www.researchgate.net/profile/Rene_Preusker/publication/268417034_Cloud_detection_with_MERIS_using_oxygen_absorption/links/553e25470cf294deef6fbae8/Cloud-detection-with-MERIS-using-oxygen-absorption.pdf
- Salem, S.A., Strand, M.H., Higa, H., Kim, H., Kazuhiro, K., Oki, K., and Oki, T. 2017. "Evaluation of MERIS chlorophyll-a retrieval processors in a complex Turbid Lake Kasumigaura over a 10-year mission." *Remote Sensing*, Vol. 9 (No. 10): pp. 1022–1043. doi:10.3390/rs9101022.
- Schroeder, T., and Fischer, J. 2003. *Atmospheric correction of MERIS imagery above case-2 waters*. Presented at the MERIS User Workshop, ESA ESRI, Frascati, Italy, 10-13 November 2003. Available at <https://pdfs.semanticscholar.org/96af/e7eef7e53820aa750eba4b820cf9875ec9a4.pdf>
- Schroeder, T., Schaale, M., and Fischer, J. 2007. "Retrieval of atmospheric and oceanic properties from MERIS measurements: A new Case-2 water processor for BEAM." *International Journal of Remote Sensing*, Vol. 28 (No. 24): pp. 5627–5632. doi:10.1080/01431160701601774.
- Seegers, B.N., Stumpf, R.P., Schaeffer, B.A., Loftin, K.A., and Werdel, P.J. 2018. "Performance metrics for the assessment of satellite data products: an ocean color case study." *Optics Express*, Vol. 26 (No. 6): pp. 7404–7422. doi:10.1364/OE.26.007404.
- Shortreed, K.S., Morton, K.F., Malange, K., and Hume, J.M.B. 2001. "Factors limiting juvenile production and enhancement potential for selected B.C. nursery lakes." DFO CSAS Research Document, 2001/098.
- Siegel, D.A., Doney, S.C., and Yoder, J.A. 2002. "The North Atlantic spring phytoplankton bloom and Sverdrup's critical depth hypothesis." *Science*, Vol. 296 (No. 5568): pp. 730–733. doi:10.1126/science.1069174.
- Stockner, J.G., and Shortreed, K.S. 1994. "Autotrophic picoplankton community dynamics in a pre-alpine lake in British Columbia, Canada." *Hydrobiologia*, Vol. 274 (No. 1–3): pp. 133–142. doi:10.1007/BF00014636.
- Strickland, J. D. H., and Parsons, T. R. 1972. *A Practical Hand Book of Seawater Analysis*. Fisheries Research Board of Canada Bulletin 157, 2nd Edition, 310 p.
- Wang, M. 2002. "The Rayleigh lookup tables for the SeaWiFS data processing: Accounting for the effects of ocean surface roughness." *International Journal of Remote Sensing*, Vol. 23 (No. 13): pp. 2693–2702. doi:10.1080/01431160110115591.
- Werdell, P.J., Franz, B.A., and Bailey, S.W. 2010. "Evaluation of shortwave infrared atmospheric correction for ocean color remote sensing of Chesapeake Bay." *Remote Sensing of Environment*, Vol. 114 (No. 10): pp. 2238–2247. doi:10.1016/j.rse.2010.04.027.